Articles

Structural Stability and Unfolding Properties of Thermostable Bacterial α-Amylases: A Comparative Study of Homologous Enzymes

J. Fitter* and S. Haber-Pohlmeier

Forschungszentrum Jülich, IBI-2: Biologische Strukturforschung, D-52425 Jülich, Germany

Received April 5, 2004; Revised Manuscript Received May 28, 2004

ABSTRACT: In a comparative investigation on two thermostable α-amylases [*Bacillus amyloliquefaciens* (BAA), $T_m = 86$ °C and *Bacillus licheniformis* (BLA), $T_m = 101$ °C], we studied thermal and guanidine hydrochloride (GndHCl)-induced unfolding using fluorescence and CD spectroscopy, as well as dynamic light scattering. Depletion of calcium from specific ion-binding sites in the protein structures reduces the melting temperature tremendously for both α-amylases. The reduction is nearly the same for both enzymes, namely, in the order of 50 °C. Thus, the difference in thermostability between BLA and BAA ($\Delta T_m \sim 15$ °C) is related to intrinsic properties of the respective protein structures themselves and is not related to the strength of ion binding. The thermal unfolding of both proteins is characterized by a full disappearance of secondary structure elements and by a concurrent expansion of the 3D structure. GndHCl-induced unfolding also yields a fully vanishing secondary structure but with more expanded 3D structures. Both α-amylases remain much more compact upon thermal unfolding as compared to the fully unfolded state induced by chemical denaturants. Such rather compact thermal unfolded structures lower the conformational entropy change during the unfolding transition, which principally can contribute to an increased thermal stability. Structural flexibilities of both enzymes, as measured with tryptophan fluorescence quenching, are almost identical for both enzymes in the native states, as well as in the unfolded states. Furthermore, we do not observe any difference in the temperature dependence of the structural flexibilities between BLA and BAA. These results indicate that conformational dynamics on the time scale of our studies seem not to be related to thermal stability or to thermal adaptation.

The unique native structure is for most proteins a basic requirement for proper functioning. It was demonstrated in many cases that the ability to build up and to keep this native and functional structure in a particular range of temperatures (as well as of pHs, pressures, and salinities) is an intrinsic property of the protein itself, which is already determined by the amino acid sequence (*1*). Surprisingly, this temperature range of the existing native structure can vary significantly for different proteins. Proteins produced by extremophilic organisms are promising candidates to perform comparative investigations to study determinants of structural stability under extreme conditions. With respect to temperature, psychrophilic (cold-adapted) and thermophilic or hyperthermophilic (heat-adapted) organisms are the most important sources of proteins (*2*, *3*). Numerous comparative studies on homologous proteins from mesophilic and thermophilic sources (*4−10*) and in some cases also from psychrophilic sources (*11−14*) have been performed. Besides small single-domain proteins with well-characterized folding and unfolding pathways and kinetics (*9*, *10*, *15−16*), some larger multidomain proteins, such as bacterial α-amylases, have been studied intensively (*8*, *11*, *14*, *17*), the latter also because

of their biotechnological relevance as amylolytic enzymes (*2*, *18*). In the case of α-amylases, various different approaches have already been applied to elucidate the origins and mechanisms of thermostability and thermal adaptation (*11*, *14*, *19−22*). In particular investigations, focusing on the interplay of enzymatic activity, structural stability, and structural flexibility was elucidative to obtain a more detailed picture about possible mechanisms of thermal adaptation (*8*, *11*, *14*). Several studies on psychrophilic, mesophilic, and thermophilic α-amylases (*11*, *14*) [but also with other homologues enzymes (*12*, *13*, *23*)] supported the concept of "corresponding states", with thermolabile pychrophilic proteins showing much more pronounced structural flexibility as compared to their mesophilic and thermophilic counterparts at the same temperature. All of theses studies report an intrinsic structural flexibility or a less compact structure, which are anticorrelated with the thermostability. Moreover, these proteins show a similar structural flexibility and enzymatic activity at their individual temperature of adaptation (corresponding state hypothesis) (*17*, *24*). In the past, we have performed studies on two α-amylases, one from the mesophilic organisms *Bacillus amyloliquefaciens* (BAA)[1] and another one from the mesophilic *Bacillus licheniformis* (BLA) but with a significant higher melting temperature

* To whom correspondence should be addressed. Phone: +49-2461-612036. Fax: +49-2461-612020. E-mail: j.fitter@fz-juelich.de.
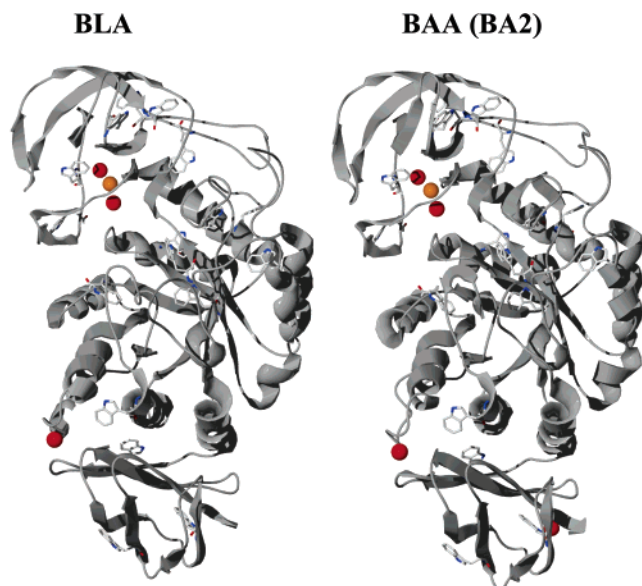
BLA   **BAA (BA2)**

FIGURE 1: Three-dimensional structure of BLA [PDB entry 1BLI (*25*)] and the best known approximation of the BAA structure (BA2, a chimeric fusion construct of α-amylase consisting of residues 1−300 from BAA and 301−483 from BLA (*26*), PDB entry 1E43). For both structures, calcium (red color) and sodium (orange color) ions are important for structural stability. With respect to fluorescence spectroscopy, it is important to note that in both structures 17 tryptophan residues have identical positions in the primary sequence, visible here by more or less identical locations and orientations in the corresponding 3D structures.

($\Delta T_m \sim 15$ °C) (*8, 19, 21*). BLA with a T_m above 100 °C is therefore denoted as a thermophilic (or even as a hyperthermophilic) protein. A comparison between both structures reveals a very high sequence homology [81% identity and 88% similarity (*25*)] accompanied by nearly identical compositions of secondary structure elements and highly corresponding three-dimensional structures (see Figure 1). As known from numerous examples of thermostable proteins, cofactors, such as iron, iron−sulfur clusters, or other ions, play an essential role for thermostability and for folding/ unfolding pathways. In the case of many α-amylases, as for BLA and BAA, calcium and sodium are required to attain thermostable protein structures (*8, 11, 25, 27*). With respect to the relationship between activity, structural flexibility, and thermal stability, our previous comparative studies on BAA and BLA did not support the concept of corresponding states (*8*). In contrast to other studies with α-amylases (*11, 14, 28*), we observed structural fluctuations that are rather similar or slightly more pronounced for the thermophilic BLA as compared to the mesophilic BAA. More pronounced fluctuations of BLA were assumed to play a role for entropic stabilization of the folded state (*19, 21*). The discrepancies between different studies on α-amylases and further differing results from various studies on other proteins in this direction (*29−31*) indicate that the impact of structural protein fluctuations on the enzymatic activity and on the mechanism of thermal adaptation is still not clarified.

---

[1] Abbreviations: BLA, *Bacillus licheniformis* α-amylase; BAA, *Bacillus amyloliquefaciens* α-amylase; DLS, dynamic light scattering; CD, circular dichroism; T_m, melting temperature; ΔH_m, enthalpy change upon thermal unfolding; ΔS_m, entropy change; ΔG_{unf}, Gibbs free energy change; Mops, 3-(*N*-morpholino)propanesulfonic acid; EDTA, ethylenediaminetetraacetic acid; GndHCl, guanidine hydrochloride.

In the past, we have analyzed structural flexibility mainly by measuring fast (picosecond) equilibrium fluctuations for the folded (*19*) and unfolded state (*21, 32*) by using neutron spectroscopy. Now, we extend our studies on BAA and BLA by measuring slower conformational fluctuations with the help of tryptophan fluorescence quenching studies. With respect to tryptophan fluorescence measurements, the pair of BLA and BAA is an excellent example for comparative studies, because the number and positions of tryptophan residues are highly conserved in both structures (see Figure 1). In addition, we also employed circular dichroism (CD) spectroscopy and dynamic light scattering (DLS) to follow changes in the secondary structure elements and to measure the compactness of both structures during the unfolding process. The goal of these studies with complementary techniques is to obtain more details about unfolding mechanisms and the thermodynamic parameter of the unfolding transition and their impact on thermostability.

EXPERIMENTAL PROCEDURES

Enzymes. Bacterial α-amylase from BLA (58 550 Da, purchased from Sigma−Aldrich) and from BAA (58 403 Da, purchased from Fluka) obtained as a lyophilized powder was dissolved in a buffer (for details see below) and was purified by the use of desalting columns (Econo-Pac 10 DG, Bio-Rad). Various spectroscopic studies were performed to compare the unfolding transition induced by temperature and chemical denaturants, as well as a function of the calcium concentration. For this purpose, the following buffers were used: 30 mM Mops, 50 mM NaCl, 2 mM $CaCl_2$ at pH 7.4 (standard buffer) and 30 mM Mops, 50 mM NaCl, 2−5 mM EDTA at pH 7.4 (calcium-free samples). In the case of CD spectroscopy, respective buffers were used but with 10 mM Mops.

Fluorescence Spectroscopy. Intrinsic fluorescence mainly caused by tryptophan and tyrosine residues was measured using a RF-1501 fluorospectrometer (Shimadzu) and a LS55 luminescence spectrometer (Perkin−Elmer). In general, excitation wavelengths of 280 and 295 nm for tryptophan quenching were applied, and emission spectra were recorded in the range between 300 and 450 nm. All fluorescence emission spectra were corrected for background scattering as measured with a pure buffer. In some cases, a UG1 filter (Schott) was used to attenuate the exciting beam, to avoid photobleaching, and to obtain most reproducible fluorescence emission spectra. Temperature scans between 10 and 115 °C with scan rates between 0.2 and 1 °C/min were performed using a constant-temperature cuvette holder connected to an external constant-temperature circulator/bath (F25, Julabo). Protein solutions (protein concentrations = 0.05 mg/mL, ∼8 $\times 10^{-7}$ mol/L) were filled into quartz cuvettes with an optical path length of 1 cm (104F-QS, Hellma).

Unfolding Transition. Thermal transition curves were obtained, either from the emission intensity at the initial peak position (peak at the lowest temperature), or from the peak position itself as a function of the temperature. Intensity data were normalized using the pre- and post-transition baseline slopes (see ref *33*).

Unfolding Kinetics. Buffer solutions were placed in the spectrometer for 5−10 min to reach thermal equilibrium at the desired temperature, before a small amount of concen-

trated protein solution was rapidly added during permanent stirring and data acquisition was started. The dead time of this procedure was about 10 s.

Dynamic Quenching of Tryptophan Fluorescence. Accessibility for external quencher molecules (acryl amide) and fluorescence quenching of tryptophan residues was measured as a function of acryl amide concentrations. This technique is well-established to investigate structural integrity and flexibility of protein structures (see ref *34*). The classical relation employed to describe the collisional quenching process is given by the Stern−Volmer equation

$$F_0/F = 1 + K_{SV}[Q] \qquad (1)$$

Here, F_0 and F are fluorescence intensities at appropriate emission wavelengths in the absence and the presence of quencher molecules. The collisional quenching constant K_{SV} gives the slope of the intensity ratio as a function of the quencher concentration $[Q]$. A correction factor was applied for the attenuation of exciting light intensity caused by acryl amide in the protein solution ("inner filter" effect with a molar absorption coefficient of 0.23 M^{-1} cm^{-1} for acryl amide at 295 nm).

CD. CD spectra in the far-UV region (200−280 nm) were recorded on a Jasco J-810 equipped with peltier thermostating cuvette holder under a constant nitrogen flow. The spectra were recorded in a 0.2-cm cell using a protein concentration of 0.13 mg/mL, averaged over three scans, and finally corrected for the buffer signal. Thermal unfolding transitions were monitored by measuring the CD signal at 222 nm at different temperatures (20−115 °C) with heating rates between 0.2 and 1 °C/min. The raw data were normalized to sample concentrations and corrected for pre- and post-transition slopes.

DLS. DLS measurements have been performed using an Ar^+ laser (Spectra physics, series 2120) operating at 488 nm with a power of 100 mW and a standard DLS instrument from ALV with an ALV 5000 E correlator (ALV Langen, Germany). All experiments were carried out at a scattering angle of 40°, a temperature of 25 °C, and a protein concentration of 2−3 mg/mL. The cuvettes have been carefully cleaned, and the samples were filtered through 200-nm Anotop filters to exclude dust. In general, DLS measures the intensity autocorrelation function $G_2(\tau)$, which is related to the electric field autocorrelation function by the Siegert equation

$$G_2(\tau) = A(1 + b|g_1(\tau)|^2) \qquad (2)$$

Here, A, b, and $|g_1(\tau)|$ are the background, a coherence factor, and the normalized electric-field autocorrelation function, respectively. For a monodisperse system in dilute solution, this correlation function is related to the translational diffusion coefficient D_T by

$$g_1(\tau) = \exp(-D_T q^2 \tau) \qquad (3)$$

where q is the scattering vector defined as $q = (4\pi n/\lambda) \sin \theta/2$, with the refractive index n, the laser wavelength λ, and the scattering angle θ. For polydisperse samples, the electric-field correlation function can be analyzed to yield information on the distribution of the relaxation times using the inverse Laplace transformation as implemented in CONTIN (*35*).

It should be noted here, that the results have been cross-validated by fitting multiexponential functions to the measured correlation function $g_1(\tau)$. Both results agree very well. According to the Stokes−Einstein equation, D_T is related to the hydrodynamic radius R_h of an equivalent sphere in the following way

$$D_T = kT/6\pi\eta R_h \qquad (4)$$

where k is the Boltzmann constant and η is the viscosity of the solvent at temperature T. Because of the low protein concentration of 3.4×10^{-5} mol/L, the mean distance between two molecules is approximately 10-fold the distance of their radius and no concentration dependence on the protein concentration is expected. For the comparison of proteins measured in a native buffer and in a buffer with 6 M guanidine hydrochloride (GndHCl), the respective refractive indices (*36*) and viscosities (*37*) have been taken into consideration and the corresponding intensity-weighted size distributions are plotted.

RESULTS

Equilibrium Thermal Unfolding. Both α-amylases are monomeric structures characterized by three distinct domains, domain A (a central (β/α) barrel), domain B (upper part of the structure), and domain C (lower part of the structure) (see Figure 1). The positions of calcium and sodium indicate the importance of these ions as stabilizing cofactors. Both structures reveal a calcium−sodium−calcium metal triade located in the interface between domains A and B, which is assumed to be essential for structural integrity and enzymatic activity. The position of the third calcium, located in the interface between domains A and C, also indicates an essential role for structural stability. The role of a fourth calcium, only found in domain C of BAA, is not clear (*26*). To investigate the impact of calcium on the secondary and 3D structure unfolding, we performed CD- and fluorescence-spectroscopy measurements on samples with 2 mM $CaCl_2$ (occupied calcium-binding sites) and with 2 mM EDTA (depleted calcium-binding sites). The experimental data for calcium-saturated samples are given in Figure 2 (data are shown only for BAA). The far-UV CD spectra are dominated by typical α-helix features, which almost fully disappear above T_m (Figure 2A). In accordance with CD spectra, the tryptophan fluorescence reveals a nearly identical thermal transition. The fluorescence emission intensity, peaked at approximately 335 nm for the native state, shows a typical decrease of the signal intensity with an increasing temperature (Figure 2B). The fluorescence emission, originating from fully and partially exposed tryptophan residues of a protein, depends on solvent properties even in absence of conformational changes. Therefore, at higher temperatures, we generally measure reduced fluorescence intensities because of a more pronounced quenching efficiency of the solvent. At the unfolding transition, we observe an additional decrease of the signal intensity and a characteristic red-shift of the emission peak (to $\lambda_{max} = \sim$340 nm). Such red shifts, which were observed for many proteins during the unfolding process, are caused by an increased solvent accessibility of

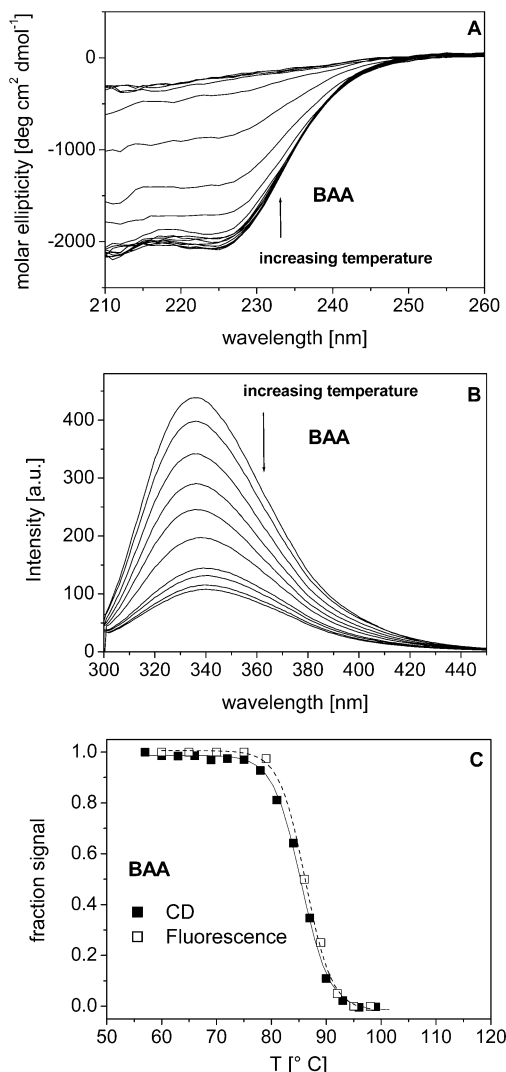FIGURE 2: Comparison of thermal unfolding transitions measured with (A) CD and (B) fluorescence spectroscopy. For both α-amylases (only BAA data are shown here), the unfolding transition occurs rather cooperative, showing more or less simultaneous unfolding (C) of the 3D structure (fluorescence spectroscopy) and secondary structure elements (CD spectroscopy).

tryptophan residues. For both enzymes, the thermal unfolding transitions (T_m = 85 ± 1 °C for BAA and 102 ± 1 °C for BLA), as measured for the secondary structure elements, coincide with the 3D structure unfolding (Figure 2C). Thermal transition measured with calcium-depleted samples revealed much lower melting temperatures (T_m = 38 ± 1 °C for BAA and 51 ± 1 °C for BLA) but exhibited the same cooperativeness with respect to secondary and 3D structure unfolding (see Figure 3A and Table 1). The tremendous shift of melting temperatures caused by calcium depletion (∼50 °C) was already observed in previous studies (8, 11) [similar effects were also observed for other α-amylases (38−40)] and is very similar for both enzymes. Although calcium exerts this strong influence on the thermal stability of both enzymes, the specific difference in thermostability between both α-amylases (ΔT_m ∼ 15 °C) is not related to calcium binding but is an intrinsic property of the protein structures. In addition to the strong calcium effect on the thermostability, we also observed a reduced thermostability in buffers without sodium but with calcium. In this case, we obtained melting temperatures T_m = 80 °C for BLA and T_m = 66 °C for BAA
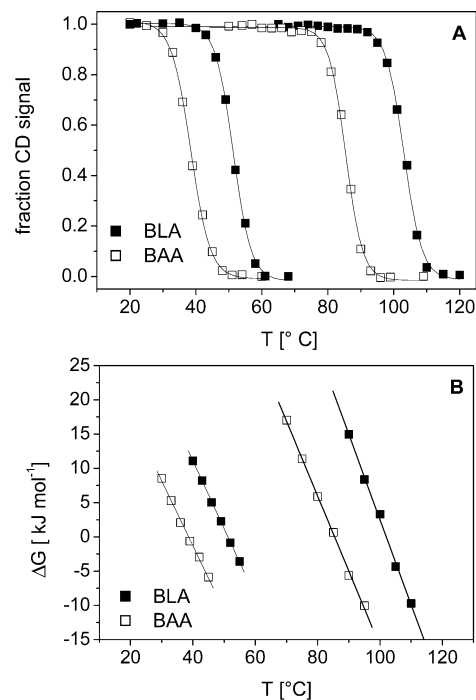

FIGURE 3: (A) Thermal unfolding transitions as measure with CD spectroscopy for samples with 2 mM EDTA (transition region = 30−60 °C) and 2 mM CaCl$_2$ (transition region = 80−110 °C). (B) In the transition region, the linear temperature dependence of ΔG_{unf} = $\Delta H - T\Delta S = -RT$ ln(f_U/f_F) was used to determine the corresponding thermodynamic parameter as given in Table 1.

Table 1: Thermodynamic Parameter of α-Amylase Thermal Unfolding

	BAA		BLA	
	Ca	EDTA	Ca	EDTA
		Fluorescence		
T_m (°C)	86	37	101	52
		CD		
T_m (°C)	85	38	103	51
ΔH_m (kJ mol^{-1})	392	294	466	319
ΔS_m (kJ mol^{-1} K^{-1})	1.095	0.947	1.242	0.985
		DSC[a]		
T_m (°C)	86		103	
ΔH_m (kJ mol^{-1})	1412		1521	
ΔS_m (kJ mol^{-1} K^{-1})	3.93		4.04	

[a] DSC data taken from ref 8.

(data not shown here). Similar reduced melting temperatures for BAA and BLA samples with sodium free-buffers were already observed earlier (41).

A comparison of van't Hoff enthalpies as determined from CD data (see Figure 3B and Table 1) and the calorimetric thermodynamic parameter taken from previous studies (8) reveals a $\Delta H_{vH}/\Delta H_{cal} < 1$, which is indicative for a non-two-state unfolding process. Although the transition curves (Figure 2C and Figure 3A) appear homogeneous with a single step and in parallel for CD and fluorescence, this characteristic is not unexpected for large multidomain proteins and was already observed in previous studies (11). Furthermore, the thermal unfolding does not show any reversibility with respect to secondary structure unfolding and only a moderate blue shift of the fluorescence emission spectrum, indicating a partial reversibility of the 3D structure unfolding (for more details see the next section).
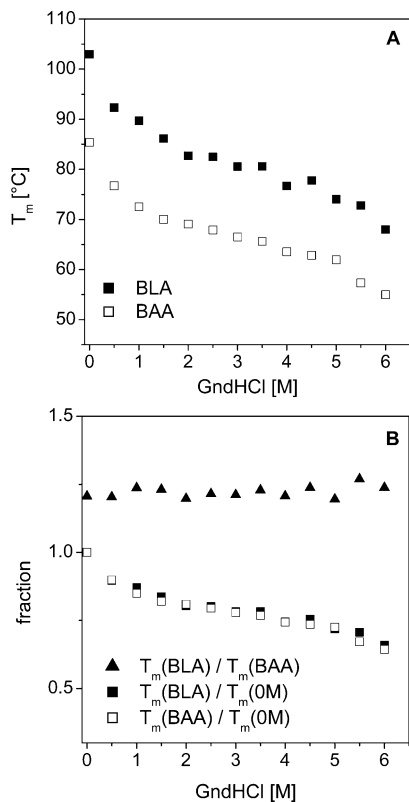
FIGURE 4: (A) T_m measured as a function of the GndHCl concentration. For both enzymes, T_m values were obtained by CD spectroscopy using samples with 2 mM CaCl$_2$. The enzymes were kept for 2 h in the respective buffers before starting the measurements. T_m is significantly decreased by an increasing concentration of the chemical denaturant for both enzymes. (B) This figure demonstrates that the GndHCl concentration dependence on T_m is nearly identical for both enzymes, although BLA shows absolute melting temperatures, which are approximately 20% larger as compared to those of BAA.

As known from many studies, thermostable proteins often exhibit a high resilience against unfolding induced by chemical denaturants such as urea and GndHCl (for examples, see refs *10*, *42*). We have performed unfolding studies with samples incubated in different concentrations of GndHCl using CD spectroscopy. For calcium-saturated samples, we observe a pronounced decrease of melting temperatures with increasing GndHCl concentrations (Figure 4A). During the time period of sample preparation and measurements (~4 h), neither BLA nor BAA fully unfolds below 6 M GndHCl at room temperature. Interestingly, the decrease of melting temperatures as a function of the GndHCl concentration is very similar for both α-amylases (Figure 4B). The difference of $\Delta T_m \sim 15$ °C as observed for buffers without chemical denaturants, remains constant (within the limits of error) for all concentrations of GndHCl. This observation indicates that, in equilibrium thermal unfolding, GndHCl has qualitatively a rather similar effect on structure destabilization for both enzymes (comparative to the stabilizing effect of calcium). For samples with GndHCl concentrations above 1 M, we already observe a small decrease of the CD signal at room temperature (with respect to the native structure without GndHCl), which suggests that a partial unfolding process takes place already at low temperatures. The nonlinear behavior of T_m as function of the denaturant concentration (Figure 4A) is a further indication for a multistep unfolding process.
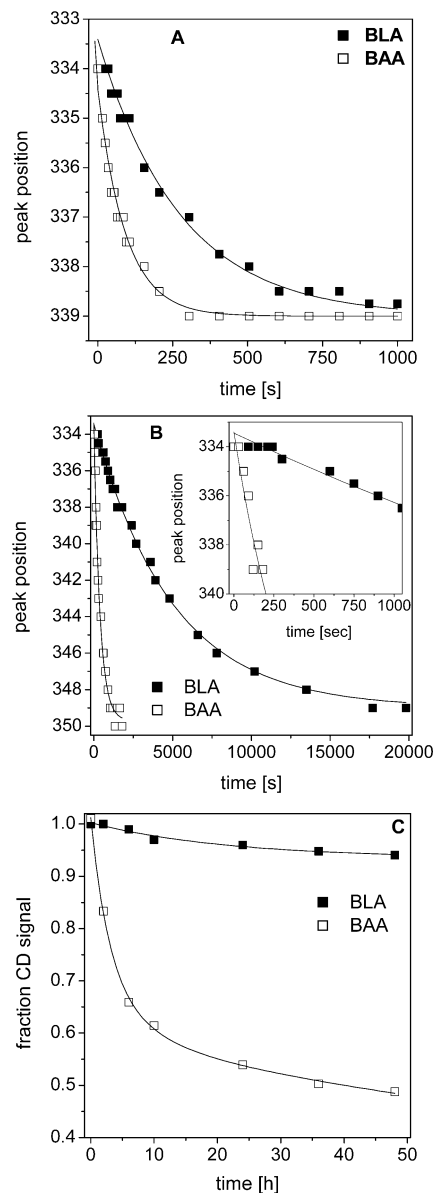

FIGURE 5: Unfolding kinetics of samples with 2 mM EDTA measured with fluorescence spectroscopy (for unfolding rates, see Table 2). (A) Thermal unfolding at 65 °C without chemical denaturants. (B) GndHCl-induced unfolding with 8 M GndHCl at 20 °C. Inset: enlarged presentation of the initial unfolding phase as given in B. (C) Long-term stability of samples with 2 mM EDTA measured with CD spectroscopy at 25 °C. In contrast to BLA, which unfolds marginally over 2 days (~5%; unfolding rate = 0.58 × 10^{-1} h^{-1}), BAA shows a significant structural unfolding (~41%; unfolding rate = 0.27 h^{-1}) in an initial phase and further but shows slower unfolding (~59%; unfolding rate = 4.13 × 10^{-3} h^{-1}) in a second phase.

Unfolding Kinetics and Unfolded States. For a detailed understanding of how proteins achieve stability, it is not only important to study the native structures of the proteins, but also the unfolded structures. To determine whether temperature- and chemical-denaturant-induced unfolding leads to the same unfolded states, we performed fluorescence measurements as a function of time (Figure 5). The comparison between temperature-induced (calcium-depleted samples at $T = 65$ °C, Figure 5A) and denaturant-induced (calcium-depleted samples with 8 M GndHCl at $T = 20$ °C, Figure 5B) unfolding reveals a striking difference in the underlying unfolding process. For both enzymes, temperature-induced

Table 2: Parameter of α-Amylase Unfolding Kinetics

	BLA		BAA	
	unfolding rate k_u (s^{-1})	half-live times $t_{1/2}$ (min)	unfolding rate k_u (s^{-1})	half-live times $t_{1/2}$ (min)
$T = 65\,°C$, 0 M GndHCl	3.65×10^{-3}	3.37	1.09×10^{-2}	1.13
$T = 20\,°C$, 8 M GndHCl	2.0×10^{-4}	61.2	2.59×10^{-3}	4.7

unfolding leads to fluorescence emission intensities with λ_{max} ~ 339 nm. In contrast to this, denaturant unfolding displays a more complete unfolding for both α-amylases, with fluorescence emission peaks around 349 nm. Although thermal unfolding exhibits fully unfolded secondary structure elements, the 3D structure remains more compact as compared to GndHCl-induced unfolding with tryptophan residues more exposed to the solvent (for more details, see Figure 6). The thermal unfolding transition seems to be limited to this red shift of $\Delta\lambda_{max}$ ~ 5 nm. Even after incubation for 2 h at elevated temperatures, we do not observe any further increase of $\Delta\lambda_{max}$. In all kinetic studies, BLA unfolding is characterized by significant smaller unfolding rates as compared to BAA (see Table 2). Chemical denaturants and high temperatures appear to have different effects with different strengths on the unfolding of both enzymes. BAA shows a partial unfolding with a similar red shift of $\Delta\lambda_{max}$ ~ 5 nm for thermal- and denaturant-induced unfolding after approximately 250 s (see part A and inset of part B of Figure 5). In contrast, BLA exhibits a red shift of 5 nm after 1000 s upon thermal unfolding and a less pronounced red shift of only 2 nm in the same time range upon denaturant-induced unfolding. For both α-amylases, the unfolding kinetics is well-characterized by a single-exponential decay and we do not observe an accumulation of intermediate states during the unfolding process. An analysis of the long-term stability of calcium-depleted samples (but without chemical denaturants) revealed a progressive unfolding of BAA even at room temperature (see Figure 5C). In contrast, BLA remains more or less folded (95% after 2 days) under the same conditions. Interestingly, in this time regime, we clearly observe a two-step unfolding of BAA (see caption of Figure 5).

As shown in Figure 6 the fluorescence emission spectra demonstrate that qualitatively the unfolding process and a partial refolding are very similar for BLA and BAA (parts A and B of Figure 6). Thermal unfolding is characterized by a rather small red shift $\Delta\lambda_{max} = 4-5$ nm, while denaturant unfolding reveals a much larger red shift of about 15 nm. To analyze the reversibility of both unfolding processes, we have measured the thermal unfolded proteins after cooling them down to room temperature. Denaturant unfolded proteins were transferred in a native buffer (without denaturants), and spectra were measured immediately after the transfer. Interestingly, for both enzymes, refolding from thermal- and denaturant-induced unfolding leads to identical emission spectra. With respect to the folded state, the spectra from the refolded state show a rather small red shift of 2−3 nm. This suggests that the refolded states are rather compact. Corresponding CD spectra show no (or very weak in the case of refolding from GndHCl unfolded states) secondary structure elements. As known from previous studies (for example, see ref *10*), we also observe a much faster refolding
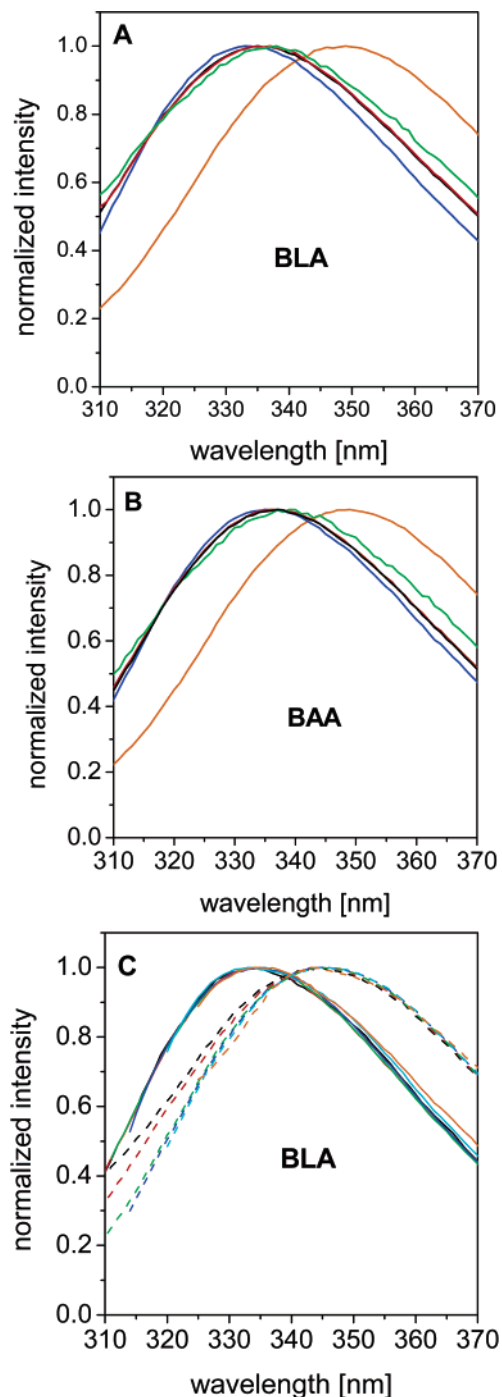

FIGURE 6: (A and B) Normalized fluorescence emission spectra for the folded and several unfolded states of α-amylase as measured with with $\lambda_{exc} = 280$ nm. Native folded state = blue line; 8 M GndHCl-induced unfolded (fully unfolded) = orange line; temperature-induced unfolded state = green line; refolded from GndHCl unfolded state = red line; and refolded from temperature unfolded state = black line. (C) Normalized fluorescence emission spectra for folded and unfolded states of BLA. Emission spectra for the folded (—) und fully unfolded (- - -) state obtained at different excitation wavelengths: $\lambda_{exc} = 275$ nm (black lines); $\lambda_{exc} = 280$ nm (red lines); $\lambda_{exc} = 290$ nm (green lines); $\lambda_{exc} = 295$ nm (blue lines); $\lambda_{exc} = 300$ nm (cyan lines); and $\lambda_{exc} = 305$ nm (orange lines).

process from GndHCl unfolded samples as compared to the unfolding process. The refolding appears as a fast "hydrophobic" collapse into compact structures, which takes place within seconds (or even faster) and is rather similar for both α-amylases.

A direct comparison of both enzymes for the native, partial (thermal), and fully unfolded states reveal rather similar spectral properties for their respective states. A small blue shift for all spectra from BLA is observed as compared to BAA. The emission spectrum obtained from a tryptophan–tyrosin mixture (L-tryptophan and L-tyrosine with a molar ratio of 1:1.75, the same ratio as in both amylases) nearly concurs with the spectra of the fully unfolded states of both enzymes. This gives evidence that only these states are characterized by more or less fully accessible tryptophan and tyrosine residues. It is well-known that for multi-tryptophan proteins the fluorescence emission spectra are depending on the excitation wavelength and therefore may differ slightly. This generally occurs because the individual tryptophan residues are located in different local environments in the native state (for example, see ref *43*). A similar behavior is visible for both α-amylases by using excitation wavelengths between 275 and 305 nm (see example of BLA in Figure 6C). A comparison of the folded state (—) to the unfolded state (- - -) exhibits emission spectra where this spectral spread nearly vanishes. However, the emission spectra of the unfolded state as measured with excitation wavelengths of 275 and 280 nm show a significantly larger intensity in the region below 330 nm, which is caused by tyrosine fluorescence. Tyrosine fluorescence emission ($\lambda_{max} \sim 305$ nm) is not observed in protein fluorescence for many native proteins (in particular, larger proteins with numerous tryptophan and tyrosine residues), because the spatial vicinity of tyrosine and tryptophan residues in the protein structure gives rise to a distinct energy transfer from tyrosine to tryptophan (see ref *43*). As a consequence, we mainly observe tryptophan fluorescence emission, although tryosine fluorescence is excited. Upon unfolding, tyrosine fluorescence emission can be visible because the less compact structure leads to increased averaged distances between tryptophan and tyrosine residues, which gives rise to observable tyrosine fluorescence emission. The tyrosine fluorescence emission can therefore be indicative for the compactness of the protein structure in different unfolded states. With respect to BLA and BAA, this effect is rather similar for both enzymes. For the thermal unfolded structures (data not shown), we already see an increase of tyrosine fluorescence emission, but it is less pronounced as compared to the fully unfolded states.

Dynamic Quenching of Fluorescence. To measure structural flexibility and integrity for both protein structures, we employed acryl amide quenching of tryprophan fluorescence. Stern–Volmer plots for BLA and BAA are shown for the native state at 20 and 40 °C in Figure 7A. While the quenching exhibits a more or less constant increase in the low-concentration region up to 100 mM, a moderate downward curve is visible over the whole region up to 600 mM. This behavior is typical for a multi-tryptophan protein with heterogeneous fluorescence, related to residues having a different accessibility to the quencher (for details, see refs *34*, *43*). Both proteins show within the limits of error identical quenching behavior and identical temperature dependence. While, for the folded state, the Stern–Volmer plots are slightly curved downward, the unfolded states (see Figure 7B) are characterized by linear or upward curved plots (compare to the solid line obtained from linear fits from the low-concentration region). The latter is indicative for samples
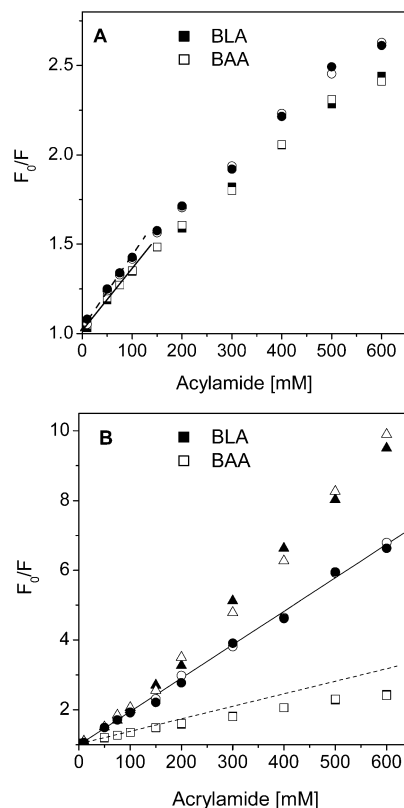

FIGURE 7: Stern–Volmer plots of tryptophan fluorescence quenching by acryl amide. (A) Native proteins were measured with 2 mM CaCl at 20 °C (■ and □) and 40 °C (● and ○). The collisional quenching constant K_{SV} values determined in the region up to 100 mM are given by the slope of the fitting line (3.37 M^{-1} at 20 °C and 3.84 M^{-1} at 40 °C). (B) Detailed comparison between quenching of folded (■ and □), partly unfolded (● and ○), and fully unfolded (▲ and △) states is shown here for 20 °C. Although partly unfolded (with 6 M GndHCl for BAA after 5 h and BLA after 24 h) and fully unfolded (both with 8 M GndHCl after 3 h) samples (all with 2 mM EDTA) differ in the region of high acryl amide concentrations, the collisional quenching constant (K_{SV} = 9.59 M^{-1} at 20 °C, obtained in the region up to 100 mM) is the same for fully and partly unfolded states.

with residues equally accessible for the quencher molecules as expected for fully unfolded samples. Furthermore, both unfolded states are characterized by significantly increased collisional quenching constants as compared to the folded state (see caption of Figure 7). Similar to the native states, we do not observe any significant difference between BLA and BAA for the unfolded states.

DLS. The hydrodynamic radius (R_h) and the size distribution of the α-amylases were obtained from DLS measurements. Figure 8 shows the intensity-weighted size distribution of diffusing proteins for the native (N), partially unfolded (I), and fully unfolded (U) states. Obviously, we observe for all states not only monomeric proteins, but also a fraction of aggregates with much larger hydrodynamic radii (around 30 nm for BAA and 80 nm for BLA) as compared to monomeric proteins. This was already visible in the experimental correlation functions, which exhibit a multimodal decay. Although the aggregated fraction appears in the distribution plot with a sizable amplitude, one has to consider that the scattered intensity is proportional to the third power of the hydrodynamic radius with respect to the mass distribution. As a consequence of this, we observe the
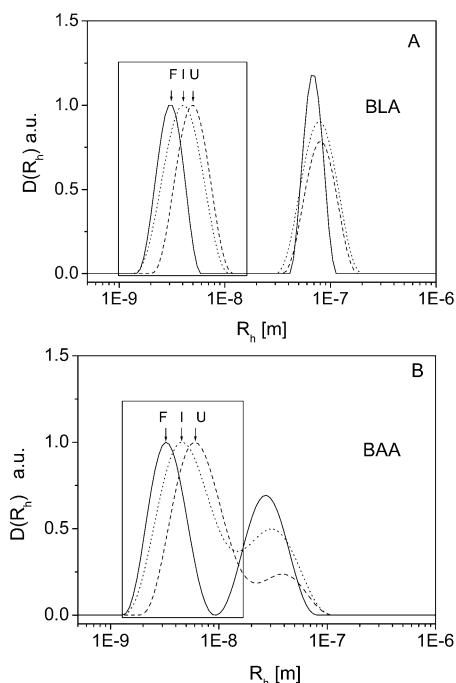
FIGURE 8: Distribution functions of the hydrodynamic radius $D(R_h)$ obtained from inverse Laplace transformation of the intensity correlation functions. The intensity-weighted size distribution with proteins in the native (F state, —), the partially unfolded (I state, ····), and the fully unfolded (U state, - - -) state as measured with DLS at 25 °C is given for (A) BLA and (B) BAA.

corresponding amplitude although the mass fraction of these aggregates is very small (~0.1%) compared to monomeric proteins. Furthermore, we observe generally broader distribution peaks for monomeric BAA as compared to BLA. This is caused by a more pronounced tendency of protein aggregation (small aggregates such as dimers, trimers, etc.) for BAA. However, for both α-amylases, we obtain the same hydrodynamic radius R_h of 3.2 ± 0.2 nm for the native monomeric structure. Considering a nonspherical (but prolate) shape of the α-amylases and a codiffusing hydration shell, the obtained values are reasonable with respect to the size of a protein consisting of 483 residues. Under unfolding conditions (6 M GndHCl and with calcium depletion), we observe a progressive expansion of both α-amylase structures with time. The fully unfolded structures are characterized by R_h = 5.2 ± 0.4 nm for BLA and about 6.1 ± 0.4 nm for BAA. On the basis of comparative studies on various denatured proteins, a relation between the number of residues and the hydrodynamic radius of unfolded proteins was estimated (*44−46*). With respect to this estimation, our radii are rather similar for BAA and noticeably smaller for BLA as compared to calculated radii for fully unfolded α-amylase structures.[2] Thermal unfolding studies bear heavily aggregated proteins, which circumvent the determination of hydrodynamic radii for monomeric proteins. Therefore, we measured R_h for partly unfolded structures exhibiting a fluorescence red shift of $\Delta\lambda_{max} \sim 4-5$ nm, equal to the value we observe for thermal unfolded structures. For these states,

we measured hydrodynamic radii of 4.0 ± 0.3 nm for BLA and 4.6 ± 0.4 nm for BAA. In contrast to the folded state, both unfolded states appear more expanded in the case of BAA as compared to BLA. Furthermore, we observe a significant increase of the distribution width for both enzymes upon unfolding. This is caused mainly by two reasons. First, a stronger tendency of aggregation with samples in the unfolded states gives rise to a peak broadening in the direction of larger radii. Second, a further peak broadening (in both directions, toward smaller and larger radii) is related to more heterogeneous structures, which are characteristic for unfolded proteins.[3]

DISCUSSION

With respect to the thermal stability, the comparison of BLA and BAA yields a difference in the melting temperature of $\Delta T_m \sim 15$ °C. This difference is observed on one hand by the use of various techniques measuring the unfolding transition (with fluorescence- and CD-spectroscopy, DSC, and activity measurements; see also ref *8*). On the other hand, under very different buffer conditions, either with stabilizing ingredients (calcium and sodium) or with destabilizing denaturants (GndHCl), the same ΔT_m was measured. All of these observations emphasize that the difference in the thermal stability between BLA and BAA is related to intrinsic properties of the protein structures themselves. There is no evidence that the strength or other properties of ion binding contributes to the difference in thermostablity between both α-amylases. The difference in thermostability between BLA and BAA is accompanied by slower unfolding rates of BLA as compared to BAA. They differ by a factor of 3 for thermal unfolding at 65 °C without chemical denaturants. Although smaller unfolding rates at a given temperature are not necessarily related to higher thermal stability,[4] slower unfolding rates are often observed for thermophilic proteins as compared to mesophilic homologues (*10, 15*). In the case of a reversible two-state unfolding process, both unfolding and refolding rates can yield equilibrium ΔG_{unf} values. In principle, these ΔG_{unf} values as measured as a function of the temperature represent stability curves (*47*), which can be very helpful to elucidate mechanisms of thermostability (*5, 7, 16, 48*). Unfortunately, here, we are dealing with a nonreversible unfolding process, which most likely is characterized by intermediate states. Therefore, the thermodynamic interpretation (for example, in terms of stability curves) of equilibrium unfolding measurements is not straightforward and has to consider intermediate states, which are accumulated at a significant level (for example, see ref *48*). In contrast to thermal unfolding, unfolding caused by high denaturant concentrations (8 M) exhibits a much more pronounced difference in unfolding rates between both α-amylases (factor 13). This observation may suggest a qualitative difference in the unfolding process as compared to thermal unfolding. A further distinct difference in the unfolding process between thermal- and denaturant-induced

---

[2] For a random coil conformation without disulfide bonds, the following relationships and corresponding hydrodynamic radii can be calculated for our α-amylase with n = 483 (number of residues): R_h = 0.655(130n/6)$^{0.5}$ [Å] = 67 Å = 6.7 nm (*44*); R_h = 2.8$n^{0.5}$ [Å] = 61.5 Å = 6.15 nm (*45*).

[3] Both effects are best visible in size distribution plots with a linear scale for the hydrodynamic radii.

[4] Gibbs free energy $\Delta G_{unf}(T)$ at a given temperature T depends not only on the unfolding rate $k_u(T)$, but also on the folding rate $k_f(T)$, with $\Delta G_{unf}(T) = -RT \ln(k_u(T)/k_f(T))$.

Table 3: Properties of Different States during the Unfolding and Refolding Process[a]

	folded, native state (F)	partially, thermal-induced unfolded state (I)	fully unfolded state (U)	partially refolded state (R)
		Fluorescence		
λ_{max} (nm)	334/335	337−339/338−340	348−349/349−350	335/336
K_{SV} (M^{-1})	3.37	9.59	9.59	
		DLS		
R_h (nm)	3.2	4.0/4.6	5.2/6.1	
secondary structure	native, folded	fully unfolded	fully unfolded	mainly or fully unfolded
3D structure	native, folded	partially unfolded	fully unfolded	collapsed, compact

[a] Parameters separated by a slash gave corresponding values for BLA and BAA. If only one value is given, the parameters are the same within the limits of error for both enzymes.

unfolding is given by the corresponding red shifts of the fluorescence emission spectra, which are much smaller for thermal unfolding. From our data, we do not have evidence that upon thermal unfolding an intermediate (or partly unfolded) state with a smaller red shift is accumulated, which might be passed through upon denaturant-induced unfolding. In this case, we would expect unfolding kinetics with a multiexponential decay. However, we measured kinetics for GndHCl-induced unfolding, which is characterized by a single-exponential decay. Furthermore, because of the fact that calorimetric and van't Hoff enthalpies differ significantly, there is evidence that already the thermal unfolding is characterized by unfolding intermediates. However, a deeper and more detailed understanding of the unfolding process requires additional measurements.

Besides the distinct differences of the individual thermostabilities and the corresponding unfolding rates, the properties of the unfolding process and of the unfolded states are qualitatively rather similar for both enzymes. This observation is supported by a summary of parameters characterizing the sequence of occurring states (see Table 3). The most noticeable difference between both enzymes is given by a smaller expansion of both unfolded states for BLA as compared to BAA. This difference is more pronounced in the case of hydrodynamic radii as compared to the red shifts of the tryptophan fluorescence emission. Principally, more compact unfolded states lower the (conformational) entropy change ΔS between the folded and unfolded state and can therefore have a stabilizing effect with respect to thermal unfolding (see refs *49*, *50*). Therefore, more compact unfolded states of BLA offer a reasonable feature, which can explain a higher thermal stability of BLA as compared to BAA. With respect to conformational fluctuations as measured by dynamic fluorescence quenching, the folded, partly unfolded, and fully unfolded structures show absolutely the same behavior for both proteins. In earlier studies, we have also measured much faster picosecond fluctuations of BAA and BLA in the folded as well as the unfolded state. In these studies, we observed only a slightly higher structural flexibility of the native BLA as compared to native BAA and rather similar flexibilities of both unfolded states (*19*, *21*). On the basis of these data, a lacking concordance between dynamical properties as measured with fluorescence quenching and the observed compactness of the unfolded states (most precisely determined by DLS) prevents a decisive and reliable answer about the role of theses properties for thermal stabilization in both α-amylases. Certainly, fluorescence quenching studies applied to unfolded structures can give only a rough picture about dynamical

features in the structure because in general all tryptophan residues are already more or less fully accessible to the solvent and the quenching behavior is only weakly (if ever) coupled to structural fluctuations. Therefore, more studies on well-characterized unfolded states employing more suited techniques are required to obtain detailed information on dynamical properties.

With respect to the properties of the folded state dynamics, our results do not support the hypothesis of corresponding states and the proposed ideas about the role of structural flexibilities for enzymatic activity and for protein stability with respect to thermal adaptation (*12*, *14*, *17*, *23*). An explanation for this discrepancy might be due to the fact that, in contrast to our study, all studies that observe results confirming the corresponding states hypothesis deal with proteins adapted to temperatures between 4 and 85 °C. It might be possible that the mechanisms related to the corresponding state hypothesis are mainly abundant in this temperature regime but do not play a role for achieving thermostability at extremely high temperatures. On the basis of numerous studies on thermostability of proteins, it is well-known that many other different mechanisms are utilized to achieve thermal adaptation (for example, see refs *2*, *7*, *10*, *51*). Considering the enormous variety of potential mechanisms, it is assumed that even quite often a combination of several different mechanisms plays a decisive role. A hint for another mechanism of thermal stabilization is given by the remarkable feature in our study that thermal unfolding of both enzymes shows a less pronounced expansion of the 3D structure as compared to fully unfolded structures. With respect to fluorescence emission red shifts and hydrodynamic radii, the thermal unfolding exhibits only one-third (with respect to red shifts) and only one-half (with respect to hydrodynamic radii) of the total expansion of the 3D structure as compared to that induced by GndHCl. Interestingly, a similar small red shift upon thermal unfolding was observed for another rather thermostable bacterial α-amylase (*Bacillus* species, $T_m \sim 82$ °C, $\Delta\lambda_{max} \sim 5$ nm). In contrast, a mesophilic α-amylase from *Asperillus oryzae* (Taka-amylase, $T_m \sim 65$ °C) shows a much more pronounced red shift to λ_{max} of about 345 nm with $\Delta\lambda_{max} \sim 10$ nm (data measured with buffers under calcium- and sodium-saturated conditions; Fitter et al., to be published). Similar observations with "residual native structures" in the unfolded state occurring in thermophilic proteins were reported recently (*52*−*54*). It was supposed that residual native structures in the unfolded state play a role in achieving higher thermal stabilities (*54*).

REFERENCES

1. Anfinsen, C. B. (1973) Principles that govern the folding of protein chains, *Science 181*, 223−230.
2. Vielle, C. and Zeikus, J. G. (2001) Hyperthermophilic enzymes: Sources, uses, and molecular mechanisms of thermostability, *Microbiol. Mol. Biol. Rev. 65* (1), 1−43.
3. Madigan, M. T., and Marrs, B. L. (1997) Extremophiles, *Sci. Am. 276*, 82−87.
4. Wallon, G., Kryger, G., Lovett, S. T., Oshima, T., Ringe, D., and Petsko, G. A. (1997) Crystal structures of *Escherichia coli* and *Salmonella typhimurium* 3-isopropylmalate dehydrogenase and comparison with their thermophilic counterpart from *Thermus thermophilus*, *J. Mol. Biol. 266*, 1016−1031.
5. Beadle, B. M., Baase, W. A., Wilson, D. B., Gilkes, N. R., and Shoichet, B. K. (1999) Comparing the thermodynamic stabilities of a related thermophilic and mesophilic enzyme, *Biochemistry 38*, 2570−2576.
6. Ladenstein, R., and Antranikian, G. (1998) Proteins from hyperthermophiles: Stability and enzymatic catalysis close to the boiling point of water, *Adv. Biochem. Eng./Biotechnol. 61*, 37−85.
7. Jaenicke, R., Schurig, H., Beaucamp, N., and Ostendorp, R. (1996) Structure and stability of hyperthermostable proteins: Glycolytic enzymes from hyperthermophilic bacterium *Thermotoga martitima*, *Adv. Protein Chem. 48*, 181−269.
8. Fitter, J., Herrmann, R., Dencher, N. A., Blume, A., and Hauss, T. (2001) Activity and stability of a thermostable α-amylase compared to its mesophilic homologue: Mechanisms of thermal adaptation, *Biochemistry 40*, 10723−10731.
9. Hollien, J., and Marqusee, S. (2002) Comparison of the folding processes of *T. thermophilus* and *E. coli* ribonucleases H, *J. Mol. Biol. 316*, 327−340.
10. Perl, D., Mueller, U., Heinemann, U., and Schmid, F. X. (2000) Two exposed amino acid residues confer thermostability on a cold shock protein, *Nat. Struct. Biol. 7* (5), 380−383.
11. Feller, G., d'Amico, D., and Gerday, C. (1999) Thermodynamic stability of a cold-active α-amylase from the Antarctic bacterium *Alteromonas haloplanctis*, *Biochemistry 38*, 4613−4619.
12. Collins, T., Meuwis M.-A., Gerday C., and Feller, G. (2003) Activity, stability, and flexibility in glycosidases adapted to extreme thermal environments, *J. Mol. Biol. 328*, 419−428.
13. Miyazaki, K., Wintrode, P. L., Grayling, R. A., Rubing, D. N., and Arnold, F. H. (2000) Directed evolution study of temperature adaptation in a psychrophilic enzyme, *J. Mol. Biol. 297*, 1015−1026.
14. Georlette, D., Blaise, V., Collins, T., D'Amico, S., Hoyoux, A., Marx, J.-C., Sonan, G., Feller, G., and Gerday, C. (2004) Some like it cold: Biocatalysis at low temperatures, *FEMS Microbiol. Rev. 28*, 25−42.
15. Cavagnero, S., Debe, D. A., Zhou, Z. H., Adams, M. W. W., and Chan, S. I. (1998) Kinetic role of electrostatic interactions in the unfolding of hyperthermophilic and mesophilic rubredoxins, *Biochemistry 37*, 3369−3376.
16. Shiraki, K., Nishikori, S., Fujiwara, S., Hashimoto, H., Kai, Y., Takagi, M., and Imanaka, T. (2001) Comparative analyses of conformational stability of a hyperthermophilic protein and its mesophilic counterpart, *Eur. J. Biochem 268*, 4144−4150.
17. Zavodszky, P., Kardos, J., Svingor, A., and Petsko, G. A. (1998) Adjustment of conformational flexibility is a key event in the thermal adaptation of proteins, *Proc. Natl. Acad. Sci. U.S.A. 95*, 7406−7411.
18. Vihinen, M., and Mäntsälä, P. (1989) Microbial amylolytic enzymes, *Crit. Rev. Biochem. Mol. Biol. 24* (4), 329−418.
19. Fitter, J., and Heberle, J. (2000) Structural equilibrium fluctuations in mesophilic and thermophilic α-amylase, *Biophys. J. 79*, 1629−1636.
20. Nielsen, J. E., and Borchert, T. V. (2000) Protein engineering of bacterial α-amylases, *Biochim. Biophys. Acta 1543*, 253−274.
21. Fitter, J., Herrmann, R., Hauss, T., Lechner, R. E., and Dencher, N. A. (2001) Dynamical properties of α-amylase in the folded and unfolded state: The role of thermal equilibrium fluctuations for conformational entropy and protein stability, *Physica B 301*, 1−7.
22. Linden, A., and Wilmanns, M. (2004) Adaptation of class-13 α-amylases to diverse living conditions, *ChemBioChem 5*, 231−239.
23. Georlette, D., Damien, B., Blaise, V., Depiereux, E., Uversky, V. N., Gerday, C., Feller, G. (2003) Structural and functional adaptations to extreme temperatures in psychrophilic, mesophilic, and thermophilic DNA ligases, *J. Biol. Chem. 278* (39), 37015−37023.
24. Somero, G. N. (1975) Temperature as a selective factor in protein evolution: The adaptational strategy of "compromise", *J. Exp. Zool. 194*, 175−188.
25. Machius, M., Wiegand, G., and Huber, R. (1995) Crystal structure of calcium-depleted *Bacillus licheniformis* α-amylase at 2.2 Å resolution, *J. Mol. Biol. 246*, 545−559.
26. Brzozowski, A. M., Lawson, D. M., Turkenburg, J. P., Bisgaard-Frantzen, H., Svendsen, A., Borchert, T. V., Dauter, Z., Wilson, K. S., and Davies, G. J. (2000) Structural analysis of a chimeric bacterial α-amylase: High-resolution analysis of native and ligand complexes, *Biochemistry 39*, 9099−9107.
27. Violet, M., and Meunier, J.-C. (1989) Kinetic study of the irreversible thermal denaturation of *Bacillus licheniformis* α-amylase, *Biochem. J. 263*, 665−670.
28. D'Amico, S., Marx, J.-C., Gerday, C., and Feller, G. (2003) Activity-stability relationships in extremophilic enzymes, *J. Biol. Chem. 278* (10), 7891−7896.
29. Hernandez, G., Jenney, F. E. J., Adams, M. W., and LeMaster, D. M. (2000) Millisecond time scale conformational flexibility in a hyperthermophile protein at ambient temperature, *Proc. Natl. Acad. Sci. U.S.A. 97*, 3166−3170.
30. Panasik, N., Brenchley, J. E., and Farber, G. K. (2000) Distributions of structural features contributing to thermostability in mesophilic and thermophilic α/β barrel glycosyl hydrolases, *Biochim. Biophys. Acta 1543*, 189−201.
31. Gershenson, A., Schauerte, J. A., Giver, L., and Arnold, F. H. (2000) Tryptophan phosphorescence study of enzyme flexibility and unfolding in laboratory-evolved thermostable esterases, *Biochemistry 39*, 4658−4665.
32. Fitter, J. (2003) A measure of conformational entropy change during thermal protein unfolding using neutron spectroscopy, *Biophys. J. 84*, 3924−3930.
33. Pace, C. N., and Scholtz, J. M. (1989) in *Protein Structure: A Practical Approach*, (Creighton, T. E., Ed.) pp 299−321, IRL Press, Oxford, U.K.
34. Eftink, M. R., and Ghiron, C. A. (1976) Exposure of tryptophanyl residues in proteins. Quantitative determination by fluorescence quenching studies, *Biochemistry 15* (3), 672−680.
35. Provencher, S. W. (1982) CONTIN−A general purpose constrained regularization program for inverting noisy linear algebraic and integral equations, *Comput. Phys. Commun. 27*, 229−242.
36. Nozaki, Y. (1972) The preparation of guanidine hydrochloride, *Methods Enzymol. 26*, 42−50.
37. Kawahara, K., and Tanford, C. (1966) Viscosity and density of aqueous solutions of urea and guanidine hydrochloride, *J. Biol. Chem. 241* (13), 3228−3332.
38. Igarashi, K., Hatada, Y., Ikawa, K., Araki, H., Ozawa, T., Kobayshi, T., Ozaki, K., and Iti, S. (1998) Improved thermostability of a *Bacillus* α-amylase by deletion of an arginine-glycine residue is caused by enhanced calcium binding, *Biochem. Biophys. Res. Commun. 248*, 372−377.
39. Savchenko, A., Vielle, C., Kang, S., and Zeikus, J. G. (2002) *Pyrococcus furiosus* α-amylase is stabilized by calcium and zinc, *Biochemistry 41*, 6193−6201.
40. Nielsen, A. D., Fuglsang, C. C., and Westh. P. (2003) Effect of calcium ions on the irreversible denaturation of a recombinant *Bacillus halmapalus* α-amylase: A calorimetric investigation, *Biochem. J. 373*, 337−343.
41. Khajeh, K., Ranjbar, B., Naderi-Manesh, H., Habibi, A. E., and Nemat-Gorgani, M. (2001) Chemical modification of bacterial α-amylases: Changes in tertiary structures and the effect of additional calcium, *Biochim. Biophys. Acta 1548*, 229−237.
42. Griffin, S., Higgins, C. L., Soulimane, T., and Wittung-Stafshede, P. (2003) High thermal and chemical stability of *Thermus thermophilus* seven-iron ferredoxin. Linear clusters form at high pH on polypeptide unfolding, *Eur. J. Biochem. 270*, 4736−4743.

43. Lakowicz, J. R. (1999) *Principles of Fluorescence Spectroscopy*, Kluwer Acedemic/Plenum Press, New York.

44. Tanford, C. (1968) Protein denaturation, *Adv. Protein Chem. 23*, 121−282.

45. Damaschun, G., Damaschun, H., Gast, K., and Zwirner, D., (1998) Denatured states of yeast phosphoglycerate kinase, *Biochemistry (Moscow) 63*, 259−275.

46. Wilkins, D. K., Grimshaw, S. H., Receveur, V., Dobson, C. M., Jones, J. A., and Smith, L. J., (1999) Hydrodynamic radii of native and denatured proteins measured by pulse field gradient NMR techniques, *Biochemistry 38*, 16424−16431.

47. Becktel, W. J., and Schellmann, J. A. (1987) Protein stability curves, *Biopolymers 26*, 1859−1877.

48. Motono, C., Oshima, T., and Yamagishi, A. (2001) High thermal stability of 3-isopropylmalate dehydrogenase from *Thermus thermophilus* resulting from low ΔC(p) of unfolding, *Protein Eng. 14* (12), 961−966.

49. Eggers, D. K., and Valentine, J. S. (2001) Molecular confinement influences protein structure and enhances thermal protein stability, *Protein Sci. 10*, 250−261.

50. Zhou, H.-X. (2004) Loops, linkages, rings, catenanes, cages, and crowders: Entropy-based strategies for stabilizing proteins, *Acc. Chem. Res. 37*, 123−130.

51. Machius, M., Declerck, N., Huber, R., and Wiegand, G. (2003) Kinetic stabilization of *Bacillus licheniformis* α-amylase through introduction of hydrophobic residues at the surface, *J. Biol. Chem. 278*, 11546−11553.

52. Shortle, D., and Ackermann, M. S. (2001) Persistence of native-like topology in a denatured protein in 8 M urea, *Science 293*, 487−489.

53. Klein-Seetharaman, J., Oikawa, M., Grimshaw, S. B., Wirmer, J., Duchardt, E., Ueda, T., Imoto, T., Smith, L. J., Dobson, C. M., and Schwalbe, H. (2002) Long-range interactions within a nonnative protein, *Science 295*, 1719−1722.

54. Robic, S., Guzman-Casado, M., Sanchez-Ruiz, J. M., and Marqusee, S., (2003) Role of residual structure in the unfolded state of a thermophilic protein, *Proc. Natl. Acad. Sci. U.S.A. 100*, 11345−11349.